OL Organic Letters

pubs.acs.org/OrgLett Letter

Evidence of an n_N(amide) → π^*_{Ar} Interaction in *N*-Alkyl-*N*,*N*′-diacylhydrazines

Jugal Kishore Rai Deka, Biswajit Sahariah, Sushil S. Sakpal, Arun Kumar Bar, Sayan Bagchi,* and Bani Kanta Sarma*

Cite This: *Org. Lett.* 2021, 23, 7003–7007 Read Online

ACCESS | Metrics & More | Article Recommendations | Supporting Information

ABSTRACT: 1,2-Dibenzoyl-1-*tert*-butylhydrazine (RH-5849) and related *N*-alkyl-*N*,*N*′-diacylhydrazines are environmentally benign insect growth regulators. Herein, we show that an unusual n_N(amide) → π^*_{Ar} interaction mediated by a hydrazide amide nitrogen atom plays a crucial role in stabilizing their biologically active trans−cis (t−c) rotameric conformations. We provide NMR and IR spectroscopic evidence for the presence of these interactions, which is also supported by X-ray crystallographic and computational studies.

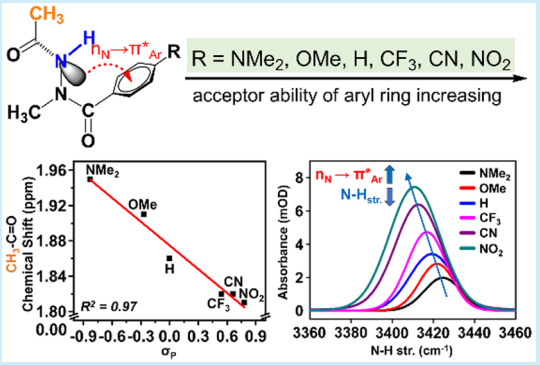

N,*N*′-Diacylhydrazines (Figure 1A) possess a wide range of biological activities. In particular, some 1,2-dibenzoyl-1-*tert*-butylhydrazine (RH-5849) (Figure 1B) analogues have been commercialized as insecticides.[1] In addition, many natural products,[2] azapeptides,[3] azatides,[4] and azapeptoids[5] contain *N*,*N*′-diacylhydrazine motifs embedded in their structure. Recently, hyperstable collagen mimetic peptides (CMPs)[6] were produced by incorporating *N*,*N*′-diacylhydrazine motifs via strategic substitution of glycines with aza-glycines in CMPs. Despite such high significance, the conformational properties of *N*,*N*′-diacylhydrazines remained poorly studied. The repulsion between the hydrazide amide nitrogen lone pairs is considered as the major driving force in determining their conformations.[7]

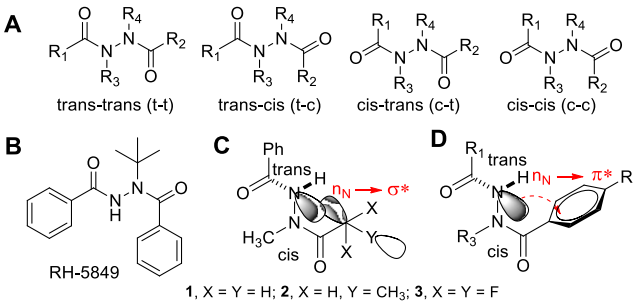

Figure 1. (A) Amide bond rotamers of *N*,*N*′-diacylhydrazines. (B) Chemical structure of RH-5849. (C) Noncovalent carbon-bonding interactions in **1**−**3** and (D) proposed n_N(amide) → π^*_{Ar} interactions in *N*-alkyl-*N*,*N*′-diacylhydrazines.

N,*N*′-Diacylhydrazines can have four amide bond rotamers (Figure 1A). In a recent study, we discussed the role of reciprocal carbonyl-carbonyl (CO···CO) n → π^* interactions in the stabilization of the trans−trans (t−t) conformations of unsubstituted *N*,*N*′-diacylhydrazines (Figure 1A, R_3 = R_4 = H).[8] We also reported that when one of the nitrogen atoms was methylated (**1**−**3**), there was a drastic conformational change and their trans−cis (t−c) conformations became more stable due to a noncovalent carbon-bonding (C-bonding) n_N(amide) → σ^*_{C-X} interaction (Figure 1C).[9] Herein, we show that incorporating a π-system such as a phenyl group at R_2 facilitates an n_N(amide) → π^*_{Ar} interaction (Figure 1D) and stabilizes the t−c conformations of *N*-alkyl-*N*,*N*′-diacylhydrazines. For example, we show that the biologically active t−c conformations of RH-5849 and its analogues that are *N*-alkylated and contain phenyl rings at the acyl positions (R_1 and R_2 of Figure 1A) are stabilized by n_N(amide) → π^*_{Ar} interactions. Understanding the noncovalent interactions that stabilize the t−c rotamers of these molecules is crucial for the *N*,*N*′-diacylhydrazine-based drug design. We provide spectroscopic evidence for the presence of this interaction in *N*-methyl-*N*,*N*′-diacylhydrazines in solution, which is also supported by X-ray crystallographic and computational studies.

Received: March 10, 2021
Published: May 11, 2021

https://doi.org/10.1021/acs.orglett.1c00834
Org. Lett. 2021, 23, 7003−7007

n → π^* has emerged as an important noncovalent interaction that can stabilize both small molecules and macromolecules.[10] However, to the best of our knowledge, there is no report of n → π^* interaction involving a nitrogen atom of amide character in the literature.

To probe the presence of the proposed n_N(amide) → π^*_{Ar} interaction, we first investigated the crystal structures of RH-5849 and its analogues from the Cambridge Structural Database (CSD) (Figures S1 and S2). These molecules (Figure 1B and 2A) crystallize in the t−c conformations in the

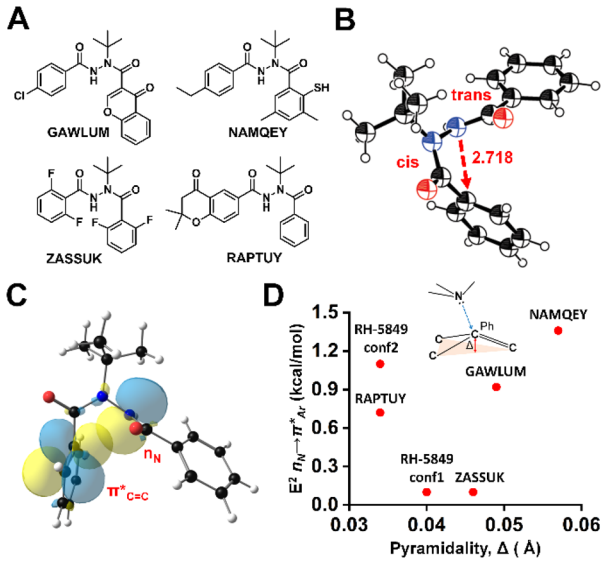

Figure 2. (A) Chemical structures of other 1,2-diaroyl-1-*tert*-butylhydrazines obtained from the CSD. (B) Crystal structure of RH-5849 (conformer 2). (C) NBO n_N(amide) → π^*_{Ar} orbital interaction in RH-5849 (conformer 2). (D) Pyramidalities of C1Ph carbon of RH-5849 and other 1,2-diaroyl-1-*tert*-butylhydrazines (Figure 2A) are plotted against their NBO n_N(amide) → π^*_{Ar} second-order perturbation energy values.

solid state with the NH−amide bonds in the trans and the NtBu−amide bonds in the cis geometries, respectively (Figure 2B and Figure S2). We observed pyramidalization of the phenyl carbon attached to the N^{t}Bu amide group (C_{1Ph}−CO) toward the NH nitrogen atom in these molecules (Figure 2C), which is a crucial evidence for the presence of n → π^* interactions.[10] Interestingly, no such trend of pyramidalization was observed in the phenyl carbon atom attached to the NH amide group [Δ(C_{2Ph}), Table 1 and Table S1]. Natural Bond Orbital (NBO) calculations also showed the presence of n_N(amide) → π^*_{Ar} interactions in these molecules (Figure 2D and Figure S3 and Table 1 and Table S1). To take the HN → CO resonance effect of the amide group into consideration, the NBO second-order perturbation energies for the n_N(amide) → π^*_{Ar} interactions were taken as 60% of the values obtained from NBO calculations as such calculations consider the amide configuration as a C=O double bond with an unconjugated nitrogen lone pair (see the Supporting Information for details). Interestingly, the stabilization energies due to the nN(amide) → π^*_{Ar} interactions in RH-5849 (1.10 kcal mol^{-1}) and its analogues are considerably higher compared to the C-bonding interaction energies in **1** and **2** (Table 1 and Table S1). The crystal structure of RH-5849 contains two molecules in the asymmetric unit.[11] In one of these molecules (RH-5849-conf1), we also observed significant CO···CO n_O → π^*_{CO}

Table 1. Crystallographic Structural Parameters and NBO Second-Order Perturbation Energies (E^2) of n_N(amide) → σ^*/π^*_{Ar} Interactions in 1−6, 4-NMe, and RH-5849

compd[a,b]	ΔC_{1Ph} (Å)	ΔC_{2Ph} (Å)	E^2 (kcal mol^{-1})[c]
1[d]		0.000	0.46
2[d]		−0.013	0.51
3[d]			
RH-5849[e]	0.034	0.009	1.10
4	0.045	−0.004	0.16
4-NMe	0.014	−0.030	1.39
5	0.041	−0.005	0.89
6	0.028	−0.032	1.08

[a]20 mM in $CDCl_3$. [b]We obtained single crystals of all these compounds except **3**. Crystal geometries were t−c. [c]n_N(amide) → π^*_{Ar} interactions calculated using crystallographic coordinates. [d]Reference 9. [e]RH-5849-conf2, data taken from ref 11 (R_4 = tBu).

interaction (1.38 kcal mol^{-1}) between the oxygen atom of NH−amide CO and the carbon atom of the NtBu−amide CO (O···C = 2.84 Å). The n_N → π^*_{Ar} interaction is considerably diminished in this molecule (0.16 kcal mol^{-1}). In addition, the cis N^{t}Bu−amide bonds in RH-5849 and its analogues are also stabilized by n_O → σ^*_{C-C} interactions between their N^{t}Bu amide CO oxygen and the $\sigma^*_{C-CH_3}$ orbital in the ^{t}Bu group (Table S1 and Figure S4).

RH-5849 and its analogues have a bulky tBu group in one of the nitrogen atoms, which could force the NtBu−amide bond to adopt cis geometry.[12] To minimize the steric effect, we substituted the tBu group with methyl (CH_3), the smallest alkyl group (**4−6**, Figure 3A). The rotameric populations of the compounds were determined by ^{1}H NMR, 1D-NOE, and 2D-NOESY experiments (see the Supporting Information). We observed only the t−c rotameric form of **4−6** in $CDCl_3$ and DMSO-d_6, wherein the NH− and NMe−amide bonds adopted trans and cis geometries, respectively. X-ray crystal

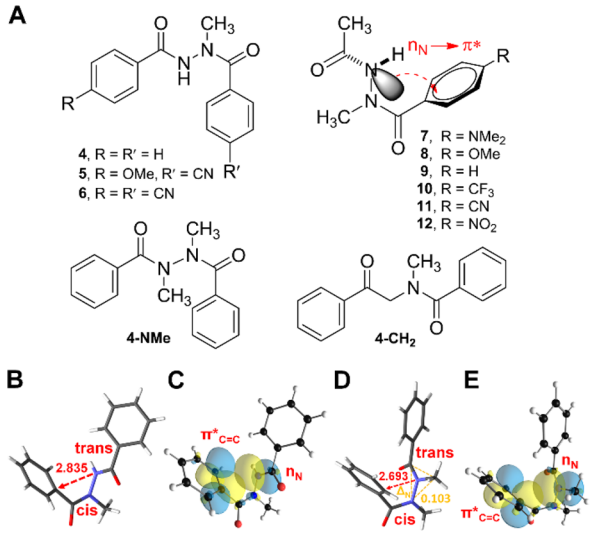

Figure 3. (A) Chemical structures of **4−12**, **4-CH$_2$**, and **4-NMe**. (B) Crystal geometry of **4**. (C) NBO orbital overlap for n_N(amide) → π^*_{Ar} interactions in **4**. (D) Crystal geometry of **4-NMe** showing the positive pyramidality (Δ_N) of the donor amidic nitrogen atom toward the Ph ring. (E) NBO orbital overlap for n_N(amide) → π^*_{Ar} interactions in **4-NMe**.

https://doi.org/10.1021/acs.orglett.1c00834
Org. Lett. 2021, 23, 7003−7007

structures of **4**−**6** also confirmed their t−c conformations in the solid state (Figure 3B and Figure S5, Tables S2 and S3).

N-Alkyl−amide bonds exist in a mixture of cis and trans rotameric forms.[13] Although the cis amide bond preference of *N*-methylanilides is known, this is a special case that arises due to the repulsion between the carbonyl oxygen lone pairs and the π-electrons of the phenyl ring on the nitrogen atom in the trans amide bond conformation.[14] We were intrigued by the complete reversal from trans (H—N—C═O ∼ 180°) to cis (Me—N—C═O ∼ 0°) geometries of the hydrazide amide bonds in **4**−**6** upon *N*-methylation. To probe this behavior, we synthesized compound **4-CH$_2$** (Figure 3A), wherein the NH group in **4** was replaced with a CH_2 isostere. Isosteric replacement of NH with CH_2 should eliminate the $n_N \rightarrow \pi^*_{Ar}$ interaction due to the absence of the electron donor lone pair in **4-CH$_2$** and should reveal the role of the $n_N \rightarrow \pi^*_{Ar}$ interaction in the conformational preference of **4**−**6**. As anticipated, we observed a mixture of cis and trans amide bond rotamers in **4-CH$_2$** (trans, 70%; cis, 30%). Therefore, it is clear that the presence of the NH group is essential for the stabilization of the cis conformations of the NMe−amide bonds in **4**−**6**. We ruled out any role of hydrogen bonding as **4-NMe** (Figure 3A) also adopted a conformation similar to that of **4** in solution and the solid state (Figure 3D). Inspection of the crystal geometries of **4**−**6** and **4-NMe** revealed positive pyramidality of the phenyl carbon (C_{Ph}) toward the NH nitrogen atom, and NBO analyses indicated the presence of n_N(amide) $\rightarrow \pi^*_{Ar}$ interactions in them (Table 1, Figure 3B−E). Interestingly, in **4-NMe**, we also observed pyramidalization of the donor nitrogen atom (0.103 Å) toward the acceptor carbon atom, indicating the presence of the n_N(amide) $\rightarrow \pi^*_{Ar}$ interaction (Figure 3D).

To systematically modulate the strength of n_N(amide) $\rightarrow \pi^*_{Ar}$ interactions and probe spectroscopic signature, we further synthesized compounds **7**−**12** (Figure 3A) with various substituents at the *para*-position of the phenyl ring. From the solution NMR studies we confirmed the t−c rotamers to be the most dominant rotamers of **7**−**12** in solution. A minor c−c rotamer was also observed due to the isomerization of the relatively smaller acetyl group to the cis form. As in **4**−**6**, no isomerization of the NMe−amide bond near the phenyl ring was observed in **7**−**12**. We could crystallize **7**−**10** and **12** (Figure 4C and Figures S5 and S6), all of which crystallized in the t−c rotameric forms with positive pyramidalization of the aromatic carbon atom (C_{Ph}) toward the amidic NH nitrogen atom (Figure 4B). Interestingly, similar to RH-5849-conf1 and RH-5849-conf2, we could crystallize **12** in two different forms (**12tc-conf1**) and (**12tc-conf2**) (Figure 4C,D). We could also locate two conformational forms (t−c-conf1 and t−c-conf2) of the t−c rotamer of **7**−**12** using quantum chemistry calculations (see the Supporting Information for details and Figure S7), which showed the dominance of the n_N(amide) $\rightarrow \pi^*_{Ar}$ interaction in the t−c-conf2 and the dominance of the CO···CO $n_O \rightarrow \pi^*_{CO}$ interaction in the t−c-conf1 conformer, respectively. This is also reflected in the higher pyramidality of the acceptor C_{Ph} atoms in the optimized geometries of the t−c-conf2 of **7**−**12** (Figure 4E, Table S7). We observed a good correlation between the N···C distances and the corresponding NBO n_N(amide) $\rightarrow \pi^*_{Ar}$ interaction energies in **7**−**12** (Figure 4F and Figure S7D). However, the effect of the n_N(amide) $\rightarrow \pi^*_{Ar}$ interaction was not observed in the change in the C—N and C═O bond lengths of the NH−amide group of **7**−**12** (Table S8).

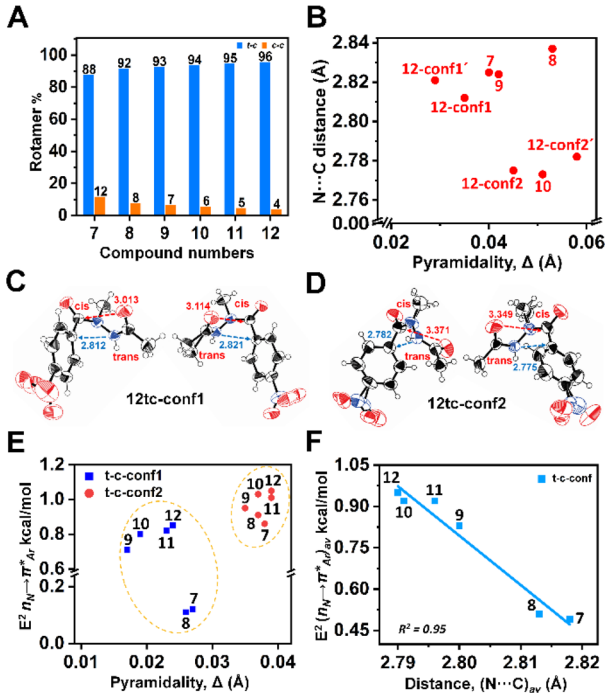

Figure 4. (A) Bar diagram showing the percentage of the rotameric populations of **7**−**12**. (B) Pyramidality of the phenyl carbon (C_{Ph}) [directly bonded to the CO group near the NMe group] observed in the crystal geometries of **7**−**10** and **12**. (C), (D) Crystal geometries of **12** in two different forms. (E) Pyramidality of the phenyl carbon (C_{Ph}) bonded to the NMe−amide group in the optimized t−c-conf1 and t−c-conf2 conformations of **7**−**12**. (F) Correlation of the N···C distances (Å) and the NBO n_N(amide) $\rightarrow \pi^*_{Ar}$ interaction energies (E^2) of **7**−**12**. The average of the N···C distances (Å) and E^2 values of the t−c-conf1 and t−c-conf2 of **7**−**12** were used for this plot (Table S7).

Interestingly, stronger $n_O \rightarrow \pi^*_{CO}$ interactions in **7**−**12** should weaken the n_N(amide) $\rightarrow \pi^*_{Ar}$ interactions and vice versa, and these two interactions should have opposite effects on the C═O and N—H stretching frequencies. $n_O \rightarrow \pi^*_{CO}$ interactions should increase the HN→CO conjugation of the donor amide and, therefore, shorten the N−H bond, and a blue shift in the N−H vibrational frequency is expected. On the other hand, n_N(amide) $\rightarrow \pi^*_{Ar}$ interactions should weaken the HN→CO conjugation of the donor amide and, therefore, elongate the N−H bond and cause a red shift in the N−H vibrational frequency. The NH stretch region of the IR spectra of **7**−**12** consisted of three overlapping peaks (Figure 5A and Figure S9A). The concentration dependent IR experiments suggested that the lowest frequency NH peak belongs to an NH that is involved in intermolecular N—H···O═C hydrogen bonding (HB) (Figure 5A), but the highest frequency peak (gray) and the middle peak (cyan) (Figure S9A) are for NH groups not involved in intermolecular HB. On the basis of NMR and IR spectroscopic observations, we assigned the highest frequency peak to the t−c and the middle peak to the c−c rotamers, respectively (see the Supporting Information for details). Analyses of the N−H vibrational frequencies of the t−c rotamers of **7**−**12** showed a gradual red shift from **7** to **12** (Figure 5B, Table S9), which indicates the dominance of n_N(amide) $\rightarrow \pi^*_{Ar}$ interactions in **7**−**12** in $CDCl_3$ solution. A strong correlation of the red shift in the N−H vibrational

https://doi.org/10.1021/acs.orglett.1c00834
Org. Lett. 2021, 23, 7003−7007

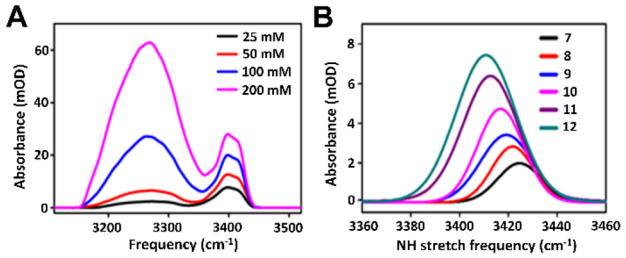

Figure 5. (A) Concentration dependent IR study of **9**. The lowest frequency population arises from intermolecular CO···NH hydrogen bonds, and thereby a nonlinear increment with concentration is observed. (B) NH vibrational frequencies of t−c rotamers of **7**−**12**. The peak positions correspond to the gray region of the peaks shown in Figure S9A that were obtained by fitting the IR spectrum of each compounds with a Gaussian + Lorentzian line shape. Details are discussed in the Supporting Information.

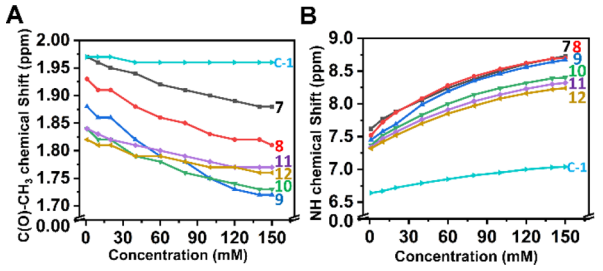

Figure 6. Concentration-dependent changes in ^{1}H NMR peaks of (A) acetyl CH_3 and (B) NH of **7**−**12** and acetohydrazide (**C-1**).

frequencies with the Hammett constant (σ_p) of the *para*-substituent (R) was observed in **7**−**12** (Figure S11A).

We also investigated the acetyl CO stretching frequencies of **7**−**12** for signatures of $n_O \rightarrow \pi^*_{CO}$ and n_N(amide) $\rightarrow \pi^*_{Ar}$ interactions. $n_O \rightarrow \pi^*_{CO}$ interactions should cause red shift of both the donor and acceptor carbonyl C═O stretching whereas n_N(amide) $\rightarrow \pi^*_{Ar}$ interactions would cause a blue shift of the acetyl C═O stretching due to weakening of the HN→CO conjugation. Analyses of the acetyl C═O stretching frequencies of the t−c conformers indicated a gradual blue hift with the increase in the electron withdrawing ability of the *para*-substituent (σ_p), which is in agreement with the expected decrease in the HN→O conjugation and increase in the C═O bond strength from **7** to **12** due to n_N(amide) $\rightarrow \pi^*_{Ar}$ interactions (Figure S11B, Table S9).

Investigation of the effect of n_N(amide) $\rightarrow \pi^*_{Ar}$ interaction on the vibrational stretching of the acceptor C═C bonds showed no gradual trend of red shift in **7**−**12**, but we observed a substantial red shift of the C═C stretching vibrations in **12** compared to that of **7** (Figure S12), which supports stronger n_N(amide) $\rightarrow \pi^*_{Ar}$ interaction in **12** compared to **7** (see the Supporting Information for details).

Further, we investigated the NMR spectroscopic signature of n_N(amide) $\rightarrow \pi^*_{Ar}$ interactions in **7**−**12**. In the absence of any other factor, we expect the electron withdrawing effect of the remote R group in the phenyl ring of **7**−**12** to shift the ^{1}H NMR signals of the NH and acetyl CH_3 groups downfield. Interestingly, however, we observed a gradual upfield shift of the ^{1}H NMR signals of both the CH_3 and NH protons of the t−c rotamers from **7** to **12** at all concentrations (1−150 mM) tested, which is evident from the inspection of relative δ values of CH_3 and NH hydrogens of **7**−**12** at various concentration points in Figure 6A,B (Table S10−S11). The Hammett correlation of the upfield shifts of the δ values of the acetyl CH_3 and NH hydrogens at 20 mM concentration with the increase in the electron withdrawing ability of the *para*-substituent (R) in the aryl ring from **7** to **12** are shown in Figure S13A,B. We reason that the increase in the n_N(amide) $\rightarrow \pi^*_{Ar}$ interaction from **7** to **12** reduces the HN → C═O conjugation, which leads to decrease in N—C double bond character and, thus, reduces the anisotropic effect of the N═C bond π-electron cloud, thereby leading to an upfield shift of the CH_3 and NH hydrogen δ values from **7** to **12**.

As hydrogen bond (HB) donation makes an amide nitrogen lone pair more available,[9] we envisaged the n_N(amide) $\rightarrow \pi^*_{Ar}$ interactions in **7**−**12** to increase with the increase in concentration. We observed a gradual upfield shift of the δ values of the CH_3 hydrogens with an increase in concentration (Figure 6A), which can be correlated to the increase in the n_N(amide) $\rightarrow \pi^*_{Ar}$ interaction and decrease in the anisotropic effect of the π-electron cloud of N═C bond with the increase in the N—H···O═C HB at higher concentration. Interestingly, in acetohydrazide (**C-1** in Figure 6A,B) that lacked the n_N(amide) $\rightarrow \pi^*_{Ar}$ interaction, no upfield shift of the acetyl CH_3 hydrogens was observed. Therefore, we conclude that the upfield shift of acetyl CH_3 hydrogens provides direct evidence of n_N(amide) $\rightarrow \pi^*_{Ar}$ interactions in **7**−**12**.

In conclusion, we have discovered a hydrazide amide nitrogen mediated n_N(amide) $\rightarrow \pi^*_{Ar}$ interaction in the insecticide RH-5849 and related *N*-alkyl-*N*,*N*′-diacylhydrazines, which stabilize their biologically active t−c rotameric conformations. As the *N*-alkyl-*N*,*N*′-diacylhydrazine motifs are found embedded in many natural products and aza-peptidomimetics, we also anticipate a role of these interactions in their stabilization.

■ ASSOCIATED CONTENT

Supporting Information

The Supporting Information is available free of charge at https://pubs.acs.org/doi/10.1021/acs.orglett.1c00834.

Experimental details, 1D, 2D, and concentration dependent NMR studies, IR studies and DFT results, synthetic protocols, crystal data, energies, structures, distance and energy graphs, NBO orbital overlaps, chemical shifts, Hammett constants and frequencies, NOESY spectra, and Cartesian coordinates (PDF)

Accession Codes

CCDC 1949085−1949087, 1956552, 2003213, 2003215−2003216, 2050118, 2050120, and 2052664 contain the supplementary crystallographic data for this paper. These data can be obtained free of charge via www.ccdc.cam.ac.uk/data_request/cif, or by emailing data_request@ccdc.cam.ac.uk, or by contacting The Cambridge Crystallographic Data Centre, 12 Union Road, Cambridge CB2 1EZ, UK; fax: +44 1223 336033.

■ AUTHOR INFORMATION

Corresponding Authors

Sayan Bagchi − *Physical and Materials Chemistry Division, CSIR-National Chemical Laboratory, Pune 411008, Maharashtra, India; Academy of Scientific and Innovative Research (AcSIR), Ghaziabad 201002, India;* orcid.org/0000-0001-6932-3113; Email: s.bagchi@ncl.res.in

https://doi.org/10.1021/acs.orglett.1c00834
Org. Lett. 2021, 23, 7003−7007

Bani Kanta Sarma − *New Chemistry Unit, Jawaharlal Nehru Centre for Advanced Scientific Research (JNCASR), Bangalore 560064, India;* orcid.org/0000-0003-0830-6007; Email: bksarma@jncasr.ac.in

Authors

Jugal Kishore Rai Deka − *Department of Chemistry, School of Natural Sciences, Shiv Nadar University, Dadri, Uttar Pradesh 201314, India*

Biswajit Sahariah − *New Chemistry Unit, Jawaharlal Nehru Centre for Advanced Scientific Research (JNCASR), Bangalore 560064, India;* orcid.org/0000-0001-6649-892X

Sushil S. Sakpal − *Physical and Materials Chemistry Division, CSIR-National Chemical Laboratory, Pune 411008, Maharashtra, India; Academy of Scientific and Innovative Research (AcSIR), Ghaziabad 201002, India*

Arun Kumar Bar − *Department of Chemistry, Indian Institute of Science Education and Research (IISER) Tirupati, Tirupati 501507, India*

Complete contact information is available at: https://pubs.acs.org/10.1021/acs.orglett.1c00834

Author Contributions

All authors have approved the final version of the manuscript.

Notes

The authors declare no competing financial interest.

■ ACKNOWLEDGMENTS

B.K.S. acknowledges the Science and Engineering Research Board (SERB), India, for research grants (ECR/2015/000337 and CRG/2019/003299) and Jawaharlal Nehru Centre for Advanced Scientific Research (JNCASR) and Shiv Nadar University (SNU) for support. J.K.R.D thanks SNU for research fellowship. S.B. acknowledges SERB (EMR/2016/000576). S.S.S. acknowledges UGC for the research fellowship.

■ REFERENCES

(1) (a) Wing, K. D. RH 5849, a nonsteroidal ecdysone agonist: effects on a Drosophila cell line. *Science* **1988**, *241* (4864), 467. (b) Carlson, G. R.; Dhadialla, T. S.; Hunter, R.; Jansson, R. K.; Jany, C. S.; Lidert, Z.; Slawecki, R. A. The chemical and biological properties of methoxyfenozide, a new insecticidal ecdysteroid agonist. *Pest Manage. Sci.* **2001**, *57* (2), 115−119.

(2) Le Goff, G.; Ouazzani, J. Natural hydrazine-containing compounds: Biosynthesis, isolation, biological activities and synthesis. *Bioorg. Med. Chem.* **2014**, *22* (23), 6529−6544.

(3) (a) Chingle, R.; Proulx, C.; Lubell, W. D. Azapeptide Synthesis Methods for Expanding Side-Chain Diversity for Biomedical Applications. *Acc. Chem. Res.* **2017**, *50* (7), 1541−1556. (b) Zega, A. Azapeptides as pharmacological agents. *Curr. Med. Chem.* **2005**, *12* (5), 589−597. (c) Avan, I.; Hall, C. D.; Katritzky, A. R. Peptidomimetics via modifications of amino acids and peptide bonds. *Chem. Soc. Rev.* **2014**, *43* (10), 3575−3594.

(4) (a) Han, H.; Janda, K. D. Azatides: Solution and Liquid Phase Syntheses of a New Peptidomimetic. *J. Am. Chem. Soc.* **1996**, *118* (11), 2539−2544. (b) Tonali, N.; Correia, I.; Lesma, J.; Bernadat, G.; Ongeri, S.; Lequin, O. Introducing sequential aza-amino acids units induces repeated β-turns and helical conformations in peptides. *Org. Biomol. Chem.* **2020**, *18* (18), 3452−3458.

(5) (a) Kanta Sarma, B.; Yousufuddin, M.; Kodadek, T. Acyl hydrazides as peptoid sub-monomers. *Chem. Commun.* **2011**, *47* (38), 10590−10592. (b) Sarma, B. K.; Kodadek, T. Submonomer Synthesis of A Hybrid Peptoid−Azapeptoid Library. *ACS Comb. Sci.* **2012**, *14* (10), 558−564. (c) Sarma, B. K.; Liu, X.; Kodadek, T. Identification of selective covalent inhibitors of platelet activating factor acetylhydrolase 1B2 from the screening of an oxadiazolone-capped peptoid−azapeptoid hybrid library. *Bioorg. Med. Chem.* **2016**, *24* (17), 3953−3963.

(6) (a) Melton, S. D.; Brackhahn, E. A. E.; Orlin, S. J.; Jin, P.; Chenoweth, D. M. Rules for the design of aza-glycine stabilized triple-helical collagen peptides. *Chem. Sci.* **2020**, *11* (39), 10638−10646. (b) Zhang, Y.; Herling, M.; Chenoweth, D. M. General Solution for Stabilizing Triple Helical Collagen. *J. Am. Chem. Soc.* **2016**, *138* (31), 9751−9754. (c) Zhang, Y.; Malamakal, R. M.; Chenoweth, D. M. Aza-Glycine Induces Collagen Hyperstability. *J. Am. Chem. Soc.* **2015**, *137* (39), 12422−12425.

(7) (a) Bishop, G. J.; Price, B. J.; Sutherland, I. O. Torsional barriers in N,N′-diacylhydrazines. *Chem. Commun.* **1967**, *14*, 672−674. (b) Kalikhman, I. D.; Bannikova, O. B.; Medvedeva, E. N.; Yushmanova, T. I.; Lopyrev, V. A. Conformational isomerism of 1,2-diformyl-, diacetyl-, and di(trifluoroacetyl) hydrazines and their methyl analogs. *Bull. Acad. Sci. USSR, Div. Chem. Sci.* **1982**, *31* (6), 1275−1277. (c) Reynolds, C. H.; Hormann, R. E. Theoretical Study of the Structure and Rotational Flexibility of Diacylhydrazines: Implications for the Structure of Nonsteroidal Ecdysone Agonists and Azapeptides. *J. Am. Chem. Soc.* **1996**, *118* (39), 9395−9401.

(8) Rahim, A.; Saha, P.; Jha, K. K.; Sukumar, N.; Sarma, B. K. Reciprocal carbonyl-carbonyl interactions in small molecules and proteins. *Nat. Commun.* **2017**, *8* (1), 78.

(9) Deka, J. K. R.; Sahariah, B.; Baruah, K.; Bar, A. K.; Sarma, B. K. Conformational control of N-methyl-N,N'-diacylhydrazines by non-covalent carbon bonding in solution. *Chem. Commun.* **2020**, *56* (36), 4874−4877.

(10) (a) Newberry, R. W.; Raines, R. T. The n→π* Interaction. *Acc. Chem. Res.* **2017**, *50* (8), 1838−1846. (b) Singh, S. K.; Das, A. The n→π* interaction: a rapidly emerging non-covalent interaction. *Phys. Chem. Chem. Phys.* **2015**, *17* (15), 9596−9612. (c) Sahariah, B.; Sarma, B. K. Spectroscopic evidence of n→π* interactions involving carbonyl groups. *Phys. Chem. Chem. Phys.* **2020**, *22* (46), 26669−26681.

(11) Chan, T. H.; Ali, A.; Britten, J. F.; Thomas, A. W.; Strunz, G. M.; Salonius, A. The crystal structure of 1,2-dibenzoyl-1-tert-butylhydrazine, a nonsteroidal ecdysone agonist, and its effects on spruce budworm (*Choristoneurafumiferana*). *Can. J. Chem.* **1990**, *68* (7), 1178−1181.

(12) (a) Roy, O.; Dumonteil, G.; Faure, S.; Jouffret, L.; Kriznik, A.; Taillefumier, C. Homogeneous and Robust Polyproline Type I Helices from Peptoids with Nonaromatic α-Chiral Side Chains. *J. Am. Chem. Soc.* **2017**, *139* (38), 13533−13540. (b) Roy, O.; Caumes, C.; Esvan, Y.; Didierjean, C.; Faure, S.; Taillefumier, C. The tert-Butyl Side Chain: A Powerful Means to Lock Peptoid Amide Bonds in the Cis Conformation. *Org. Lett.* **2013**, *15* (9), 2246−2249.

(13) Sui, Q.; Borchardt, D.; Rabenstein, D. L. Kinetics and Equilibria of Cis/trans Isomerization of Backbone amide bonds in peptoids. *J. Am. Chem. Soc.* **2007**, *129* (39), 12042−12048.

(14) (a) Yamasaki, R.; Tanatani, A.; Azumaya, I.; Saito, S.; Yamaguchi, K.; Kagechika, H. Amide conformational switching induced by protonation of aromatic substituent. *Org. Lett.* **2003**, *5* (8), 1265−1267. (b) Saito, S.; Toriumi, Y.; Tomioka, N.; Itai, A. Theoretical Studies on cis-amide preference in N-methylanilides. *J. Org. Chem.* **1995**, *60* (15), 4715−4720. (c) Itai, A.; Toriumi, Y.; Saito, S.; Kagechika, H.; Shudo, K. Preference for cis-amide structure in N-acyl-N-methylanilines. *J. Am. Chem. Soc.* **1992**, *114* (26), 10649−10650.